Subacute SARS-CoV-2 replication can be controlled in the absence of CD8$^+$ T cells in cynomolgus macaques

Short title: Subacute SARS-CoV-2 replication can be controlled without CD8$^+$ T cells

Takushi Nomura[1]*, Hiroyuki Yamamoto[1], Masako Nishizawa[1], Trang Thi Thu Hau[1], Shigeyoshi Harada[1], Hiroshi Ishii[1], Sayuri Seki[1], Midori Nakamura-Hoshi[1], Midori Okazaki[1], Sachie Daigen[1], Ai Kawana-Tachikawa[1,2,3], Noriyo Nagata[4], Naoko Iwata-Yoshikawa[4], Nozomi Shiwa[4], Shun Iida[4], Harutaka Katano[4], Tadaki Suzuki[4], Eun-Sil Park[5], Ken Maeda[5], Yuriko Suzaki[6], Yasushi Ami[6], and Tetsuro Matano[1,2,3]*

[1]AIDS Research Center, National Institute of Infectious Diseases, Tokyo, Japan

[2]Institute of Medical Science, University of Tokyo, Tokyo, Japan

[3]Joint Research Center for Human Retrovirus Infection, Kumamoto University, Kumamoto, Japan

[4]Department of Pathology, National Institute of Infectious Diseases, Tokyo, Japan

[5]Department of Veterinary Science, National Institute of Infectious Diseases, Tokyo, Japan

[6]Division of Laboratory Animal Research, National Institute of Infectious Diseases, Tokyo, Japan

*Equally-contributed corresponding authors: nomutaku@nih.go.jp (TN) and tmatano@nih.go.jp (TM)

Abstract

SARS-CoV-2 infection presents clinical manifestations ranging from asymptomatic to fatal respiratory failure. Despite the induction of functional SARS-CoV-2-specific $CD8^+$ T-cell responses in convalescent individuals, the role of virus-specific $CD8^+$ T-cell responses in the control of SARS-CoV-2 replication remains unknown. In the present study, we show that subacute SARS-CoV-2 replication can be controlled in the absence of $CD8^+$ T cells in cynomolgus macaques. Eight macaques were intranasally inoculated with 10^5 or 10^6 $TCID_{50}$ of SARS-CoV-2, and three of the eight macaques were treated with a monoclonal anti-CD8 antibody on days 5 and 7 post-infection. In these three macaques, $CD8^+$ T cells were undetectable on day 7 and thereafter, while virus-specific $CD8^+$ T-cell responses were induced in the remaining five untreated animals. Viral RNA was detected in nasopharyngeal swabs for 10-17 days post-infection in all macaques, and the kinetics of viral RNA levels in pharyngeal swabs and plasma neutralizing antibody titers were comparable between the anti-CD8 antibody treated and untreated animals. SARS-CoV-2 RNA was detected in the pharyngeal mucosa and/or retropharyngeal lymph node obtained at necropsy on day 21 in two of the untreated group but undetectable in all macaques treated with anti-CD8 antibody. $CD8^+$ T-cell responses may contribute to viral control in SARS-CoV-2 infection, but our results indicate possible containment of subacute viral replication in the absence of $CD8^+$ T cells, implying that $CD8^+$ T-cell dysfunction may not solely lead to viral control failure.

Author Summary

SARS-CoV-2 infection presents a wide spectrum of clinical manifestations ranging from asymptomatic to fatal respiratory failure. The determinants for failure in viral control and/or fatal disease progression have not been elucidated fully. Both acquired immune effectors, antibodies and $CD8^+$ T cells, are considered to contribute to viral control. However, it remains unknown whether a deficiency in either of these two arms is directly linked to failure in the control of SARS-CoV-2 replication. In the present study, to know the requirement of $CD8^+$ T cells for viral control after the establishment of infection, we examined the effect of $CD8^+$ cell depletion by monoclonal anti-CD8 antibody administration in the subacute phase on SARS-CoV-2 replication in cynomolgus macaques. Unexpectedly, our analysis revealed no significant impact of $CD8^+$ cell depletion on viral replication, indicating that subacute SARS-CoV-2 replication can be controlled in the absence of $CD8^+$ T cells. $CD8^+$ T-cell responses may contribute to viral control in SARS-CoV-2 infection, but this study suggests that $CD8^+$ T-cell dysfunction may not solely lead to viral control failure or fatal disease progression.

Introduction

The coronavirus disease 2019 (COVID-19) caused by severe acute respiratory syndrome coronavirus 2 (SARS-CoV-2) has rapidly spread resulting in a major pandemic [1]. SARS-CoV-2 transmission occurs via the respiratory route, and the average incubation period from infection to symptom onset has been estimated to be 5 days [2]. SARS-CoV-2 infection presents a wide spectrum of clinical manifestations ranging from asymptomatic to fatal respiratory failure [3]. Multiple cofounding factors such as age and underlying diseases are associated with COVID-19 severity [4-8]. For instance, auto-antibodies against type I interferon have been reported to be associated with life-threatening COVID-19 pneumonia [9,10]. However, the exact determinants for failure in viral control and/or fatal disease progression have not been elucidated fully.

Most non-fatal COVID-19 cases show a limited period of detectable virus production in pharyngeal swabs peaking at around one week post-infection [11]. Host acquired as well as innate immune responses are involved in the control of viral replication [8,12-14]. Anti-SARS-CoV-2 neutralizing antibodies are induced in most infected individuals [13-16]. Recent clinical studies including those on convalescent plasma and/or monoclonal antibody administration have indicated efficacy of neutralizing antibodies against SARS-CoV-2 infection [17-20]. Animal studies have confirmed *in vivo* efficacy of neutralizing antibodies against infection [21-25]. Also, SARS-CoV-2-specific T-cell responses are induced in most non-fatal COVID-19 cases [26-28]. Current studies have indicated induction of functional virus-specific CD8+ T-cell responses in convalescent COVID-19 individuals, implying suppressive pressure of CD8+ T cells on SARS-CoV-2 replication [29,30]. Thus, both acquired immune effectors, antibodies and $CD8^+$ T cells, are considered to contribute to viral control. However, it remains unknown whether a deficiency in either of these two arms is directly linked to failure in the control of SARS-CoV-2 replication. It has been reported that COVID-19 patients with

agammaglobulinemia controlled disease progression, suggesting viral control even in the absence of antibody responses [31].

A previous study of anti-CD8 antibody administration prior to re-infection in rhesus macaques has indicated partial contribution of CD8+ T cells to protection against SARS-CoV-2 re-infection [25]. However, the requirement of $CD8^+$ T cells for the control of virus replication after the establishment of infection remains unclear. In the present study, we investigated the effect of $CD8^+$ cell depletion by monoclonal anti-CD8 antibody administration in the subacute phase on SARS-CoV-2 replication in cynomolgus macaques. Unexpectedly, our analysis revealed no significant impact of $CD8^+$ cell depletion on viral replication, indicating that subacute SARS-CoV-2 replication can be controlled in the absence of $CD8^+$ T cells.

Results

Kinetics of SARS-CoV-2 infection in cynomolgus macaques after intranasal inoculation

Previous studies have shown that intranasal and intratracheal inoculation with 10^5 $TCID_{50}$ (50% tissue culture infective doses) of SARS-CoV-2 results in the establishment of infection in rhesus macaques, with viral RNA detectable for more than a week post-infection in pharyngeal swabs [32,33]. In the present study, we first examined whether intranasal SARS-CoV-2 inoculation only can result in viral infection in cynomolgus macaques. In the first experiment, cynomolgus macaques were intranasally inoculated with 10^6 (exactly 7.5 x 10^5 in macaque N011), 10^5 (exactly 7.5 x 10^4 in macaques N012 and N013), or 10^4 (exactly 7.5 x 10^3 in macaque N014) $TCID_{50}$ of SARS-CoV-2 (Table 1). Macaques N011, N012, and N013 showed similar levels of viral RNA in nasopharyngeal swabs on day 2, at the peak (Fig 1A). Viral RNA was also detected in throat swabs with a lower peak (Fig 1B). Viral RNA in nasopharyngeal swabs was detectable for approximately two weeks (up to: day 17 in N011, day 12 in N012, and day 14 in N013) after virus inoculation (Fig 1A, 1C, and 1D). Subgenomic RNAs (sgRNAs) were also detected in nasopharyngeal and throat swabs, indicating viral replication (Fig 2A and 2B). SARS-CoV-2 sgRNAs were detected in nasopharyngeal swabs until day 9 in N011, day 7 in N012, and day 5 in N013 (Fig 2A, 2C, and 2D). However, in macaque N014, which was inoculated with 10^4 $TCID_{50}$ of SARS-CoV-2, sgRNAs were undetectable, and viral RNAs were detectable albeit at lower levels, only until day 5 in nasopharyngeal swabs (Fig 1A and Fig 2A), indicating that 10^4 $TCID_{50}$ is below the virus inoculum threshold to consistently induce detectable viral replication. N014 was subsequently excluded from further analyses.

In the second experiment, two (N021 and D023) and three (N022, D024, and D025) macaques were intranasally inoculated with 10^6 and 10^5 $TCID_{50}$ of SARS-CoV-2, respectively (Table 1). Monoclonal anti-CD8 antibody was administered intravenously on days 5 and 7 to three (D023, D024, and D025 in Group D) of the five macaques. All of the five macaques in

the second experiment showed comparable levels of viral RNAs and sgRNAs in nasopharyngeal swabs on day 2 compared to the three macaques inoculated with 10^6 or 10^5 $TCID_{50}$ of SARS-CoV-2 in the first experiment (Fig 1A and Fig 2A). Indeed, no significant difference in RNA levels in nasopharyngeal swabs on day 5 was observed between the first three and the second five animals (Fig 1E). No clear difference in viral loads in either nasopharyngeal or throat swabs on days 2 and 5 was observed between macaques inoculated with 10^6 (n = 3) and 10^5 (n = 5) $TCID_{50}$ of SARS-CoV-2 (Fig 1C and 1D and Fig 2C and 2D). Viral RNA in nasopharyngeal swabs was detectable until day 14 in N021 and day 10 in N022 following inoculation (Fig 1A, 1C, and 1D). SARS-CoV-2 sgRNAs in nasopharyngeal swabs were detected until day 5 in N021 and day 7 in N022 following inoculation (Fig 2A, 2C, and 2D). Collectively, in the first and second experiments, intranasal inoculation of cynomolgus macaques with 10^6 or 10^5 $TCID_{50}$ of SARS-CoV-2 resulted in viral replication with viral RNA detectable for 10-17 days in nasopharyngeal swabs.

Kinetics of SARS-CoV-2 infection after $CD8^+$ cell depletion

We then investigated the effect of $CD8^+$ cell depletion on viral replication in the subacute phase of SARS-CoV-2 infection. In the three Group D macaques administered with anti-CD8 antibody on days 5 and 7, $CD8^+$ T cells were undetectable in peripheral blood on day 7 and thereafter (Fig 3). These three macaques showed comparable levels of viral RNA in nasopharyngeal swabs before (day 5) and after (day 7) anti-CD8 antibody treatment compared to the five untreated Group N macaques (Fig 1F). Viral RNA in nasopharyngeal swabs was detectable until day 10 in D025 and day 14 in macaques D023 in D024 after virus inoculation (Fig 1A, 1C, and 1D). Viral sgRNAs in nasopharyngeal swabs were detected until day 2 in D023, day 5 in D024, and day 7 in D025 (Fig 2A, 2C, and 2D). Collectively, no clear difference in viral RNA levels in swabs was observed for the three anti-CD8 antibody-treated Group D

versus the five untreated Group N macaques.

We also examined whether virus could be recovered from individual swab samples (Table 2). SARS-CoV-2 was recovered from nasopharyngeal and throat swabs from all eight animals intranasally inoculated with either 10^6 or 10^5 $TCID_{50}$. Virus was recovered for 2-12 days in anti-CD8 antibody-untreated macaques (until day 2 in N021, day 5 in N013 and N022, day 7 in N011, and day 12 in N012) and for 2-7 days in anti-CD8 antibody-treated macaques (until day 2 in D024 and day 7 in D023 and D025). There was no indication of enhanced virus recovery after CD8 cell depletion.

Macaque N021 was euthanized on day 14, while the remaining animals were euthanized on day 21 post-infection (Table 1). Examination of body temperature showed transient slight fever in some animals (on day 2 in N021 and D025; on day 6 in D023 and D024; on days 13-19 in N012) (S1 Fig). Histopathological analysis of the lung obtained at necropsy on day 14 in macaque N021 revealed mild or moderate pulmonary inflammation (S2 Fig), whereas no significant pathology in the lung was detected on day 21 in other animals.

RNA was extracted from the pharyngeal mucosa, retropharyngeal lymph nodes (RPLN), lung, intestine, and spleen obtained at necropsy, and subjected to RT-PCR for detection of viral RNA (Table 3). Viral RNA was undetectable in tissues from macaques N012, N014, N021, D023, and D024. However, viral RNA was detected in the RPLN of N011, in the pharyngeal mucosa, RPLN, and spleen of N013, and in the spleens of N022 and D025. Additionally, viral sgRNAs were also detectable in pharyngeal mucosa, RPLN, and spleen of N013. There was no evidence of enhanced viral replication in anti-CD8 antibody-treated macaques.

Antibody and T-cell responses in macaques after intranasal SARS-CoV-2 inoculation

Anti-SARS-CoV-2 neutralizing antibody (NAb) responses were induced in all the macaques after intranasal SARS-CoV-2 inoculation (Fig 4) NAb responses were detected on

day 7 in macaques N021 and D025 only, and in all animals on day 14. Macaques D025 and D024 exhibited the highest and lowest NAb titers, respectively. No clear difference in NAb responses was observed between the three anti-CD8 antibody-treated and the five untreated macaques.

Finally, we examined $CD8^+$ T-cell responses specific for SARS-CoV-2 spike (S), nucleocapsid (N), and membrane-and-envelope (M&E) antigens in the five anti-CD8 antibody-untreated macaques inoculated with 10^6 or 10^5 $TCID_{50}$ of SARS-CoV-2. In the analysis using peripheral blood mononuclear cells (PBMCs), SARS-CoV-2-specific $CD8^+$ T-cell responses were undetectable in macaque N013 but detected in the remaining four macaques (Fig 5A and 5B). Macaque N022 exhibited $CD8^+$ T-cell responses on day 7 while the remaining three macaques (N011, N012, and N021) showed initial SARS-CoV-2 specific responses on day 14. Analysis using submandibular lymph nodes (SMLN) obtained at necropsy found SARS-CoV-2-specific $CD8^+$ T-cell responses in macaques N011, N013, and N021 (Fig 5C). Interestingly, SARS-CoV-2-specific $CD8^+$ T-cell responses were undetectable in PBMCs but detected in SMLN in macaque N013. Thus, SARS-CoV-2-specific $CD8^+$ T-cell responses were detected in all the five anti-CD8 antibody-untreated Group N macaques inoculated with 10^6 or 10^5 $TCID_{50}$ of SARS-CoV-2.

Discussion

Host T-cell and B-cell responses have been reported to contribute to the control of SARS-CoV-2 replication [8,12,13,28]. In a murine model of infection with a mouse-adapted strain of SARS-CoV, depletion of CD4+ T cells resulted in reduced neutralizing antibody responses and delayed virus clearance from the lung [34]. Furthermore, SARS-CoV replication was controlled in the absence of CD4+ T and B cells, implicating CD8+ T cells in viral control [35]. Recent studies in humans have shown that functional virus-specific CD8+ T-cell responses are induced in convalescent COVID-19 individuals [29,30]. These reports suggest contribution of $CD8^+$ T cells in the control of SARS-CoV-2 replication. However, it remains unclear whether SARS-CoV-2 replication can be controlled in the absence of $CD8^+$ T cells. In the present study, we investigated the impact of depletion of $CD8^+$ cells (including $CD8^+$ T cells) by anti-CD8 antibody administration on SARS-CoV-2 replication in the subacute phase after establishment of virus infection. We found no significant enhancement of viral replication or delay in viral clearance after $CD8^+$ cell depletion, indicating that subacute SARS-CoV-2 replication can be controlled in the absence of $CD8^+$ T cells.

Our findings do not deny the contribution of $CD8^+$ T cells in the control of SARS-CoV-2 replication or the possibility of viral protection by vaccine-induced $CD8^+$ T cells. What is indicated in the present study is that $CD8^+$ T-cell dysfunction is not directly linked to failure in viral control, possibly implying that there may be multiple arms of host immune mechanisms involved in containing SARS-CoV-2 replication.

An animal model for SARS-CoV-2 infection is necessary for analysis of pathogenesis and transmission and the evaluation of vaccines and anti-viral drugs. Non-human primate models are recognized as being the most clinically relevant because of their genetic and physiological similarities to humans. Recent studies have shown that rhesus and cynomolgus macaques can be infected with SARS-CoV-2 and exhibit clinical manifestations resembling

human COVID-19 [32,36-38]. Both macaque species present mild to moderate forms of COVID-19, which is observed in the majority of the human population. We thus used a model of SARS-CoV-2 infection in cynomolgus macaques for analysis of the effect of $CD8^+$ cell depletion on virus replication.

We attempted SARS-CoV-2 inoculation via the intranasal route only without intratracheal inoculation, because it may more closely reflect viral transmissions in humans. The geometric means of peak viral RNAs and sgRNAs in nasopharyngeal swabs (on day 2) were 2.7×10^8 (range: 1.1×10^8 to 5.2×10^8) and 1.0×10^6 (range: 1.8×10^5 to 1.8×10^6) copies/swab, respectively, which are equivalent to those in rhesus macaques inoculated both intranasally and intratracheally with 10^5 $TCID_{50}$ of SARS-CoV-2 [32,33]. In macaques inoculated with 10^5 $TCID_{50}$ (1.4×10^8 RNA copies) of SARS-CoV-2, viral RNA copies in nasopharyngeal swabs on day 2 were comparable (N012) to or greater (N013, N022, D024, and D025) than the total viral RNA copies in the inoculum, confirming viral replication in macaques even with 10^5 $TCID_{50}$. The three macaques inoculated with 10^6 $TCID_{50}$ showed similar levels of viral RNA in nasopharyngeal swabs on days 2 and 5 compared to the five macaques with 10^5 $TCID_{50}$. All the eight macaques intranasally inoculated with 10^6 or 10^5 $TCID_{50}$ of SARS-CoV-2 developed efficient anti-SARS-CoV-2 NAb responses, and the five anti-CD8 antibody-untreated macaques induced SARS-CoV-2-specific $CD8^+$ T-cell responses. Taken together, our results show that intranasal inoculation of cynomolgus macaques with 10^6 or 10^5 $TCID_{50}$ of SARS-CoV-2 results in viral replication in the pharyngeal mucosa. Containment of viral replication in the pharyngeal mucosa would be important for the control of further viral transmission as well as disease progression.

Our cynomolgus macaque model of intranasal but not intratracheal SARS-CoV-2 inoculation is considered to represent asymptomatic or mild COVID-19. However, histopathological analysis of the lung detected pulmonary inflammation in one animal (N021)

236 on day 14 post-infection (S2 Fig), suggesting the potential of intranasal SARS-CoV-2
237 inoculation to induce moderate pulmonary diseases. Other animals may also have developed
238 mild pulmonary inflammation detectable on day 14, which was resolved by day 21. Macaque
239 N013 showed a unique phenotype with undetectable viral RNAs in swabs after day 14 (Fig 1D)
240 but relatively higher levels of viral RNA in pharyngeal mucosa and submandibular lymph nodes
241 on day 21 post-infection (Table 3). Virus-specific $CD8^+$ T-cell responses were undetectable in
242 PBMCs but efficiently detected in the submandibular lymph nodes on day 21 (Fig 5),
243 suggesting localized virus replication in the pharyngeal mucosa.

244 The sample size used in this study is relatively limited (three anti-CD8 antibody treated
245 animals and five untreated controls). However, these three animals exhibited similar levels of
246 pharyngeal viral loads before the anti-CD8 antibody treatment, and again showed similar levels
247 of viral loads after $CD8^+$ cell depletion. Neither enhancement of viral replication nor delay in
248 viral control was observed. Therefore, this study provides sufficient evidence for our conclusion.

249 In summary, the present study showed that subacute SARS-CoV-2 replication can be
250 controlled even in the absence of $CD8^+$ T cells. In SARS-CoV-2 infection, $CD8^+$ T-cell
251 responses may contribute to viral control, but our results suggest that $CD8^+$ T-cell dysfunction
252 does not solely lead to viral control failure or disease progression.
253

Materials and Methods

Ethics statement

Animal experiments were performed in the National Institute of Infectious Diseases (NIID) after approval by the Committee on the Ethics of Animal Experiments in NIID (permission number: 520001) under the guidelines for animal experiments in accordance with the Guidelines for Proper Conduct of Animal Experiments established by the Science Council of Japan (http://www.scj.go.jp/ja/info/kohyo/pdf/kohyo-20-k16-2e.pdf). The experiments were in accordance with the "Weatherall report for the use of non-human primates in research" recommendations (https://royalsociety.org/topics-policy/publications/2006/weatherall-report/). Each macaque was housed in a separate cage and received standard primate feed and fresh fruit daily. Virus inoculation, blood collection, nasopharyngeal and throat swab collection, and anti-CD8 antibody treatment were performed under ketamine anesthesia. Macaques were euthanized by whole blood collection under deep anesthesia on day 14 or 21 post-infection.

Animal experiments

SARS-CoV-2 wk-521 strain [39] (2019-nCoV/Japan/TY/WK-521/2020, GenBank Accession LC522975) was expanded in Vero E6/TMPRSS2 cells [39] and harvested to prepare a virus inoculum stock. Virus infectivity was assessed by detection of cytopathic effect (CPE) on Vero E6/TMPRSS2 cells and determination of endpoint titers. Nine cynomolgus macaques (*Macaca fascicularis*, 3-6 years old) were intranasally inoculated with the same stock of SARS-CoV-2 wk-521 at a dose of 10^6 (exactly 7.5×10^5) $TCID_{50}$ (1.4×10^9 RNA copies) (n = 3), 10^5 (exactly 7.5×10^4) $TCID_{50}$ (n = 5), or 10^4 (exactly 7.5×10^3) $TCID_{50}$ (n = 1) (Table 1). Three (Group D) of the nine macaques were intravenously administrated with 5 mg/kg body weight of anti-CD8α antibody clone MT807 (NIH Nonhuman Primate Reagent Resource) on days 5 and 7 post-infection. Body temperature was measured with a small implantable thermo logger

(DST micro-T; Star-Oddi) that was set intraperitoneally under ketamine anesthesia at least five days prior to virus inoculation. Macaques were euthanized and subjected to necropsy on day 14 or 21 post-infection (Table 1).

Detection of SARS-CoV-2 RNAs

Swab RNA was extracted from 0.2 ml of swab solutions (1ml of DMEM with 2% fetal bovine serum [Cytiva]) using QIAamp Viral RNA Minikit (QIAGEN) and subjected to real-time RT-PCR for viral RNA quantitation [40] using QuantiTect Probe RT-PCR Kit (Qiagen) and QuantStudio 5 (Thermo Fisher Scientific). Swab RNAs were also subjected to real-time RT-PCR for measurement of viral subgenomic RNA (sgRNA) levels [32,33,41] using the following primers: SARS2-LeaderF60 (5'-CGATCTCTTGTAGATCTGTTCTCT-3'), SARS2-N28354R (5'-TCTGAGGGTCCACCAAACGT-3'), and SARS2-N28313Fam (FAM-TCAGCGAAATGCACCCCGCA-TAMRA). Tissue RNAs were extracted from homogenized tissues by using TRIzol™ Plus RNA Purification Kit (Thermo Fisher Scientific) with phenol-chloroform extraction and subjected to real-time RT-PCR for detection of viral RNAs.

Virus recovery from swabs

Vero E6/TMPRSS2 cells in 96-well plates were added with 10-fold serially diluted swab solutions and cultured for 4 days without medium change. Virus recovery was assessed by detection of CPE and determination of endpoint titers. Swab samples with virus titers greater than 1 x 10^2 $TCID_{50}$/swab were considered positive.

Analysis of anti-SARS-CoV-2 NAb responses

Plasma samples were heat inactivated for 30 min at 56 °C. Serial two-fold dilutions of heat-inactivated plasma were tested in quadruplicate. In each mixture for quadruplicate testing,

304 40 µl of diluted plasma were incubated with 40 µl of 80 $TCID_{50}$ SARS-CoV-2 wk-521. After
305 incubation for 45 min at room temperature, 20 µl of the mixture was added to each of four wells
306 (1 x 10^4 Vero cells/well) in a 96-well plate. Three days later, virus infectivity was assessed by
307 detection of CPE to determine the endpoint titers. The lower limit of detection was 1:10.
308
309 **Analysis of cell surface markers**
310 Whole blood samples were treated with Lysing Solution (BD) and subjected to surface
311 staining using anti-CD3 APC-Cy7 (SP34-2; BD), anti-CD4 FITC (M-T477; BD), anti-CD8
312 PerCP (SK1; BD), and anti-CD20 PE (2H7; BD) antibodies. Alternatively, whole blood
313 samples from anti-CD8 antibody-treated animals were stained with anti-CD3 APC-Cy7, anti-
314 CD4 PerCP (L200; BD), anti-CD8 FITC (DK25; FUJIFILM), and anti-CD20 PE. Stained cells
315 were analyzed by BD FACS Canto II.
316
317 **Analysis of SARS-CoV-2 antigen-specific $CD8^+$ T-cell responses**
318 Virus-specific $CD8^+$ T-cell frequencies were measured by flow cytometric analysis of
319 gamma interferon (IFN-γ) induction after specific stimulation as described previously [42].
320 PBMCs were prepared from whole blood by density gradient centrifugation using Ficoll-Paque
321 PLUS (Cytiva). Lymph node-derived lymphocytes were prepared from minced lymph nodes by
322 density gradient centrifugation using Ficoll-Paque PLUS. Cells were pulsed and cocultured
323 with peptide pools (at a final concentration of more than 0.1 µM for each peptide) using panels
324 of overlapping peptides spanning the SARS-CoV-2 S, N, M, and E amino acid sequences (PM-
325 WCPV-S-1, PM-WCPV-NCAP-1, PM-WCPV-VME-1, and PM-WCPV-VEMP-1; JPT Peptide
326 Technologies) in the presence of GolgiStop (monensin, BD), 1 µg/ml of anti-CD28 (CD28.2,
327 BD) and 1 µg/ml anti-CD49d (9F10, BD) for 6 hours. Intracellular IFN-γ staining was
328 performed with a CytofixCytoperm kit (BD) and anti-CD3 APC-Cy7, anti-CD4 FITC, anti-

CD8 PerCP, and anti-IFN-γ PE (4S.B3; BioLegend). Stained cells were analyzed by BD FACS Lyric. A representative gating schema for flow cytometric analysis is shown in Fig. 5A. Specific T-cell frequencies were calculated by subtracting nonspecific IFN-γ^+ T-cell frequencies from those after peptide-specific stimulation. Specific T-cell frequencies less than 0.03% of $CD8^+$ T cells were considered negative.

Statistical analysis

Statistical analyses were performed using Prism software (GraphPad Software, Inc.) with significance set at p values of < 0.05. Comparisons were performed by Mann-Whitney U test.

Acknowledgments

We thank S. Matsuyama and M. Takeda for providing SARS-CoV-2 wk-521 and Vero E6/TMPRSS2 cells, H. Ohashi and K. Watashi for providing Vero cells, and S. Fukushi for his help. We also thank M. de Souza for editing the paper.

References

1. World Health Organization. Situation reports. https://www.who.int/emergencies/diseases/novel-coronavirus-2019/situation-reports.
2. Wiersinga WJ, Rhodes A, Cheng AC, Peacock SJ, Prescott HC. Pathophysiology, transmission, diagnosis, and treatment of coronavirus disease 2019 (COVID-19): a review. JAMA. 2020; 324(8):782-93. doi: 10.1001/jama.2020.12839.
3. Kenny G, Mallon PW. COVID19- clinical presentation and therapeutic considerations. Biochem Biophys Res Commun. 2021; 538:125-131. doi: 10.1016/j.bbrc.2020.11.021.
4. Garg S, Kim L, Whitaker M, O'Halloran A, Cummings C, Holstein R, et al. Hospitalization rates and characteristics of patients hospitalized with laboratory-confirmed coronavirus disease 2019 - COVID-NET, 14 States, March 1-30, 2020. MMWR Morb Mortal Wkly Rep. 2020; 69(15):458-64. doi: 10.15585/mmwr.mm6915e3.
5. Richardson S, Hirsch JS, Narasimhan M, Crawford JM, McGinn T, Davidson KW, et al. Presenting characteristics, comorbidities, and outcomes among 5700 patients hospitalized with COVID-19 in the New York City area. JAMA. 2020; 323(20):2052-9.
6. Grasselli G, Zangrillo A, Zanella A, Antonelli M, Cabrini L, Castelli A, et al. Baseline characteristics and outcomes of 1591 patients infected with SARS-CoV-2 admitted to ICUs of the Lombardy Region, Italy. JAMA. 2020; 323(16):1574-81.
7. Arunachalam PS, Wimmers F, Mok CKP, Perera R, Scott M, Hagan T, et al. Systems biological assessment of immunity to mild versus severe COVID-19 infection in humans. Science. 2020; 369(6508):1210-20.
8. Blanco-Melo D, Nilsson-Payant BE, Liu WC, Uhl S, Hoagland D, Moller R, et al. Imbalanced host response to SARS-CoV-2 drives development of COVID-19. Cell. 2020; 181(5):1036-45.e9. doi: 10.1016/j.cell.2020.04.026.
9. Bastard P, Rosen LB, Zhang Q, Michailidis E, Hoffmann HH, Zhang Y, et al.

Autoantibodies against type I IFNs in patients with life-threatening COVID-19. Science. 2020; 370(6515): eabd4585. doi: 10.1126/science.abd4585.

10. Zhang Q, Bastard P, Liu Z, Le Pen J, Moncada-Velez M, Chen J, et al. Inborn errors of type I IFN immunity in patients with life-threatening COVID-19. Science. 2020; 370(6515):eabd4570. doi: 10.1126/science.abd4570.
11. Liu Y, Yan LM, Wan L, Xiang TX, Le A, Liu JM, et al. Viral dynamics in mild and severe cases of COVID-19. Lancet Infect Dis. 2020; 20(6):656-7.
12. Vabret N, Britton GJ, Gruber C, Hegde S, Kim J, Kuksin M, et al. Immunology of COVID-19: Current state of the Science. Immunity. 2020; 52(6):910-941. doi: 10.1016/j.immuni.2020.05.002.
13. Ni L, Ye F, Cheng ML, Feng Y, Deng YQ, Zhao H, et al. Detection of SARS-CoV-2-Specific humoral and cellular immunity in COVID-19 convalescent individuals. Immunity. 2020; 52(6):971-7 e3.
14. Rydyznski Moderbacher C, Ramirez SI, Dan JM, Grifoni A, Hastie KM, Weiskopf D, et al. Antigen-specific adaptive immunity to SARS-CoV-2 in acute COVID-19 and associations with age and disease severity. Cell. 2020; 183(4):996-1012 e19.
15. Wajnberg A, Amanat F, Firpo A, Altman DR, Bailey MJ, Mansour M, et al. Robust neutralizing antibodies to SARS-CoV-2 infection persist for months. Science. 2020; 370(6521):1227-30.
16. Dan JM, Mateus J, Kato Y, Hastie KM, Yu ED, Faliti CE, et al. Immunological memory to SARS-CoV-2 assessed for up to 8 months after infection. Science. 2021; 371(6529):eabf4063. doi: 10.1126/science.abf4063.
17. Garcia-Beltran WF, Lam EC, Astudillo MG, Yang D, Miller TE, Feldman J, et al. COVID-19-neutralizing antibodies predict disease severity and survival. Cell. 2021; 184:476-488.e411. doi: 10.1016/j.cell.2020.12.015.

18. Shen C, Wang Z, Zhao F, Yang Y, Li J, Yuan J, et al. Treatment of 5 Critically Ill Patients With COVID-19 With Convalescent Plasma. JAMA. 2020; 323(16):1582-9.
19. Gottlieb RL, Nirula A, Chen P, Boscia J, Heller B, Morris J, et al. Effect of Bamlanivimab as monotherapy or in combination with Etesevimab on viral load in patients with mild to moderate COVID-19: A randomized clinical trial. JAMA. 2021; 325(7):632-44.
20. Weinreich DM, Sivapalasingam S, Norton T, Ali S, Gao H, Bhore R, et al. REGN-COV2, a neutralizing antibody cocktail, in outpatients with COVID-19. N Engl J Med. 2021; 384(3):238-51.
21. Hassan AO, Case JB, Winkler ES, Thackray LB, Kafai NM, Bailey AL, et al. A SARS-CoV-2 infection model in mice demonstrates protection by neutralizing antibodies. Cell. 2020; 182(3):744-53 e4.
22. Rogers TF, Zhao F, Huang D, Beutler N, Burns A, He WT, et al. Isolation of potent SARS-CoV-2 neutralizing antibodies and protection from disease in a small animal model. Science. 2020; 369(6506):956-63.
23. Baum A, Ajithdoss D, Copin R, Zhou A, Lanza K, Negron N, et al. REGN-COV2 antibodies prevent and treat SARS-CoV-2 infection in rhesus macaques and hamsters. Science. 2020; 370:1110-1115. doi: 10.1126/science.abe2402.
24. Jones BE, Brown-Augsburger PL, Corbett KS, Westendorf K, Davies J, Cujec TP, et al. The neutralizing antibody, LY-CoV555, protects against SARS-CoV-2 infection in non-human primates. Sci Transl Med. 2021; 13(593):eabf1906. doi: 10.1126/scitranslmed.abf1906.
25. McMahan K, Yu J, Mercado NB, Loos C, Tostanoski LH, Chandrashekar A, et al. Correlates of protection against SARS-CoV-2 in rhesus macaques. Nature. 2021; 590:630-634. doi: 10.1038/s41586-020-03041-6.
26. Grifoni A, Weiskopf D, Ramirez SI, Mateus J, Dan JM, Moderbacher CR, et al. Targets of

T cell responses to SARS-CoV-2 coronavirus in humans with COVID-19 disease and unexposed individuals. Cell. 2020; 181(7):1489-501 e15.

27. Sekine T, Perez-Potti A, Rivera-Ballesteros O, Stralin K, Gorin JB, Olsson A, et al. Robust T cell immunity in convalescent individuals with asymptomatic or mild COVID-19. Cell. 2020; 183(1):158-68 e14.

28. DiPiazza AT, Graham BS, Ruckwardt TJ. T cell immunity to SARS-CoV-2 following natural infection and vaccination. Biochem Biophys Res Commun. 2021;538:211-217. doi: 10.1016/j.bbrc.2020.10.060.

29. Tan AT, Linster M, Tan CW, Le Bert N, Chia WN, Kunasegaran K, et al. Early induction of functional SARS-CoV-2-specific T cells associates with rapid viral clearance and mild disease in COVID-19 patients. Cell Rep. 2021; 34(6):108728. doi: 10.1016/j.celrep.2021.108728.

30. Kared H, Redd AD, Bloch EM, Bonny TS, Sumatoh H, Kairi F, et al. SARS-CoV-2-specific CD8+ T cell responses in convalescent COVID-19 individuals. J Clin Invest. 2021; 131(5):e145476. doi: 10.1172/JCI145476.

31. Quinti I, Lougaris V, Milito C, Cinetto F, Pecoraro A, Mezzaroma I, et al. A possible role for B cells in COVID-19? Lesson from patients with agammaglobulinemia. J Allergy Clin Immunol. 2020; 146(1):211-3 e4.

32. Chandrashekar A, Liu J, Martinot AJ, McMahan K, Mercado NB, Peter L, et al. SARS-CoV-2 infection protects against rechallenge in rhesus macaques. Science. 2020; 369(6505):812-817. doi: 10.1126/science.abc4776.

33. Mercado NB, Zahn R, Wegmann F, Loos C, Chandrashekar A, Yu J, et al. Single-shot Ad26 vaccine protects against SARS-CoV-2 in rhesus macaques. Nature. 2020; 586(7830):583-588. doi: 10.1038/s41586-020-2607-z.

34. Chen J, Lau YF, Lamirande EW, Paddock CD, Bartlett JH, Zaki SR, et al. Cellular immune

445 responses to severe acute respiratory syndrome coronavirus (SARS-CoV) infection in
446 senescent BALB/c mice: CD4+ T cells are important in control of SARS-CoV infection. J
447 Virol. 2010; 84(3):1289-301.
448 35. Channappanavar R, Fett C, Zhao J, Meyerholz DK, Perlman S. Virus-specific memory
449 CD8 T cells provide substantial protection from lethal severe acute respiratory syndrome
450 coronavirus infection. J Virol. 2014; 88(19):11034-44.
451 36. Rockx B, Kuiken T, Herfst S, Bestebroer T, Lamers MM, Oude Munnink BB, et al.
452 Comparative pathogenesis of COVID-19, MERS, and SARS in a nonhuman primate model.
453 Science. 2020; 368(6494):1012-1015. doi: 10.1126/science.abb7314.
454 37. Munster VJ, Feldmann F, Williamson BN, van Doremalen N, Pérez-Pérez L, Schulz J, et
455 al. Respiratory disease in rhesus macaques inoculated with SARS-CoV-2. Nature. 2020;
456 585(7824):268-272. doi: 10.1038/s41586-020-2324-7.
457 38. Salguero FJ, White AD, Slack GS, Fotheringham SA, Bewley KR, Gooch KE, et al.
458 Comparison of rhesus and cynomolgus macaques as an infection model for COVID-19.
459 Nat Commun. 2021; 12(1):1260. doi: 10.1038/s41467-021-21389-9.
460 39. Matsuyama S, Nao N, Shirato K, Kawase M, Saito S, Takayama I, et al. Enhanced isolation
461 of SARS-CoV-2 by TMPRSS2-expressing cells. Proc Natl Acad Sci U S A. 2020;
462 117(13):7001-7003. doi: 10.1073/pnas.2002589117.
463 40. Shirato K, Nao N, Katano H, Takayama I, Saito S, Kato F, et al. Development of genetic
464 diagnostic methods for detection for novel coronavirus 2019(nCoV-2019) in Japan. Jpn J
465 Infect Dis. 2020; 73(4):304-307. doi: 10.7883/yoken.JJID.2020.061.
466 41. Nagata N, Iwata-Yoshikawa N, Sano K, Ainai A, Shiwa N, Shirakura M, et al. The
467 peripheral T cell population is associated with pneumonia severity in cynomolgus monkeys
468 experimentally infected with severe acute respiratory syndrome coronavirus 2. bioRxiv preprint
469 doi: https://www.biorxiv.org/content/10.1101/2021.01.07.425698v1.

42. Nomura T, Yamamoto H, Ishii H, Akari H, Naruse TK, Kimura A, et al. Broadening of virus-specific CD8+ T-cell responses is indicative of residual viral replication in aviremic SIV controllers. PLoS Pathog. 2015; 11(11):e1005247. doi: 10.1371/journal.ppat.1005247.

474 **Supporting Information**

475 **S1 Fig. Changes in body temperatures pre- and post-infection in macaques.**

476

477 **S2 Fig. Histopathology of the lung in macaque N021.**

478 Representative histopathology with hematoxylin and eosin staining (H&E) of the lung obtained
479 from macaque N021 at autopsy on day 14 post-infection, indicating mild or moderate
480 pulmonary inflammation. Infiltration of mononuclear cells were observed around blood vessels
481 and bronchiole (upper left panel). Lymphocytes, eosinophils, and macrophages were observed
482 in pulmonary alveoli (upper right and lower panels).

483

Figure Captions

Fig 1. Viral RNA levels in swabs.

(A-D) Changes in viral RNA levels in nasopharyngeal (A, C, D) and throat (B) swabs after SARS-CoV-2 infection in all animals (A, B) or those infected with 10^6 (C) or 10^5 (D) $TCID_{50}$ of SARS-CoV-2. The lower limit of detection was approximately 3 x 10^3 copies/swab. (E) Comparison of viral RNA levels in nasopharyngeal swabs at day 5 post-infection between 10^6 $TCID_{50}$-infected and 10^5 $TCID_{50}$-infected macaques. No significant difference was observed. (F) Comparison of viral RNA levels in nasopharyngeal swabs at days 5 (left), 7 (middle), and 9-12 (right) post-infection between Group N and D animals infected with 10^6 or 10^5 $TCID_{50}$ of SARS-CoV-2. No significant difference was observed.

Fig 2. Viral subgenomic RNA levels in swabs.

Changes in viral sgRNA levels in nasopharyngeal (A, C, D) and throat (B) swabs after SARS-CoV-2 infection in all animals (A, B) or those infected with 10^6 (C) or 10^5 (D) $TCID_{50}$ of SARS-CoV-2. The lower limit of detection was approximately 3 x 10^3 copies/swab.

Fig 3. Peripheral blood B- and T-cell frequencies.

Changes in $\%CD3^+$, $\%CD3^+CD4^+$, $\%CD3^+CD8^+$, and $\%CD3^-CD20^+$ T cells in macaque PBMCs after SARS-CoV-2 infection.

Fig 4. SARS-CoV-2-specific neutralizing antibody responses.

Changes in plasma anti-SARS-CoV-2 neutralizing antibody titers post-infection in all animals (left) or those infected with 10^6 (middle) or 10^5 (right) $TCID_{50}$ of SARS-CoV-2.

Fig 5. SARS-CoV-2-specific $CD8^+$ T-cell responses.

509 (A) Representative gating schema for detection of IFN-γ induction after stimulation with
510 overlapping M&E peptide pools in macaque N012 on day 14 post-infection. (B) Frequencies
511 of $CD8^+$ T cells targeting S, N, and M&E in PBMCs on days 7, 14, and 21 post-infection in
512 Group N animals infected with 10^6 (middle) or 10^5 (right) $TCID_{50}$ of SARS-CoV-2. (C)
513 Frequencies of $CD8^+$ T cells targeting S, N, and M & E in submandibular lymph nodes obtained
514 at necropsy in macaques N011, N013, N021, and N022. Samples were unavailable for analysis
515 in macaque N012.
516

Table 1. Macaque experimental protocol

Group	Experiment[a]	Macaques	Gender	Age (yrs)	SARS-CoV-2 dose[b] ($TCID_{50}$)	anti-CD8 Ab Tx[c]	Necropsy[d]
N	1	N011	male	6	10^6	NT	d21
N	1	N012	male	6	10^5	NT	d21
N	1	N013	male	6	10^5	NT	d21
-[e]	1	N014	male	6	10^4	NT	d21
N	2	N021	female	3	10^6	NT	d14
N	2	N022	female	3	10^5	NT	d21
D	2	D023	male	6	10^6	d5 & d7	d21
D	2	D024	male	6	10^5	d5 & d7	d21
D	2	D025	female	3	10^5	d5 & d7	d21

[a]Two sets of experiments were performed using the same SARS-CoV-2 inoculum stock.

[b]Macaques were intranasally inoculated with the indicated doses (10^6 [exactly 7.5 x 10^5], 10^5 [exactly 7.5 x 10^4], or 10^4 [exactly 7.5 x 10^3] $TCID_{50}$) of SARS-CoV-2 on day 0.

[c]Macaques in Group D were treated intravenously with anti-CD8 antibody on days 5 and 7 post-infection. NT, not treated.

[d]Macaques were euthanized and necropsied on day 14 or 21 post-infection.

[e]N014 was excluded from comparisons between groups N and D.

526 **Table 2. Virus recovery from pharyngeal swabs after SARS-CoV-2 infection**

Macaques	Virus recovery from swabs[a]								
	d0	d2	d5	d7	d9/10	d12	d14	d17	d21
N011	-	+	+	+	-	-	-	-	-
	-	+	+	-	-	-	-	-	-
N012	-	+	+	+	-	+	-	-	-
	-	+	-	-	-	-	-	-	-
N013	-	+	-	-	-	-	-	-	-
	-	+	+	-	-	-	-	-	-
N014	-	-	-	-	-	-	-	-	-
	-	+	-	-	-	-	-	-	-
N021	-	+	-	-	-	-	-	-	-
	-	+	-	-	-	-	-	-	-
N022	-	+	+	-	-	-	-	-	-
	-	+	-	-	-	-	-	-	-
D023	-	+	-	+	-	-	-	-	-
	-	+	-	-	-	-	-	-	-
D024	-	+	-	-	-	-	-	-	-
	-	+	-	-	-	-	-	-	-
D025	-	+	+	+	-	-	-	-	-
	-	+	+	-	-	-	-	-	-

527 [a]Swab samples were added to Vero-E6 cell culture to recover infectious virus. + indicates
528 successful virus recovery from nasopharyngeal (upper row) or throat (lower row) swabs for
529 each animal.
530

Table 3. Detection of viral RNA in tissues obtained at necropsy

Macaques	Autopsy	Detection of viral RNA in tissues[a]				
		Pharyngeal mucosa	Retropharyngeal lymph node	Lung	Intestine	Spleen
N011	d21	-	+	-	-	-
N012	d21	-	-	-	-	-
N013	d21	+	+	-	-	+
N014	d21	-	-	-	-	-
N021	d14	-	-	-	-	-
N022	d21	-	-	-	-	+
D023	d21	-	-	-	-	-
D024	d21	-	-	-	-	-
D025	d21	-	-	-	-	+

[a]RNA was extracted from individual tissues and subjected to RT-PCR to detect SARS-CoV-2 RNA. + indicates detection of viral RNA.

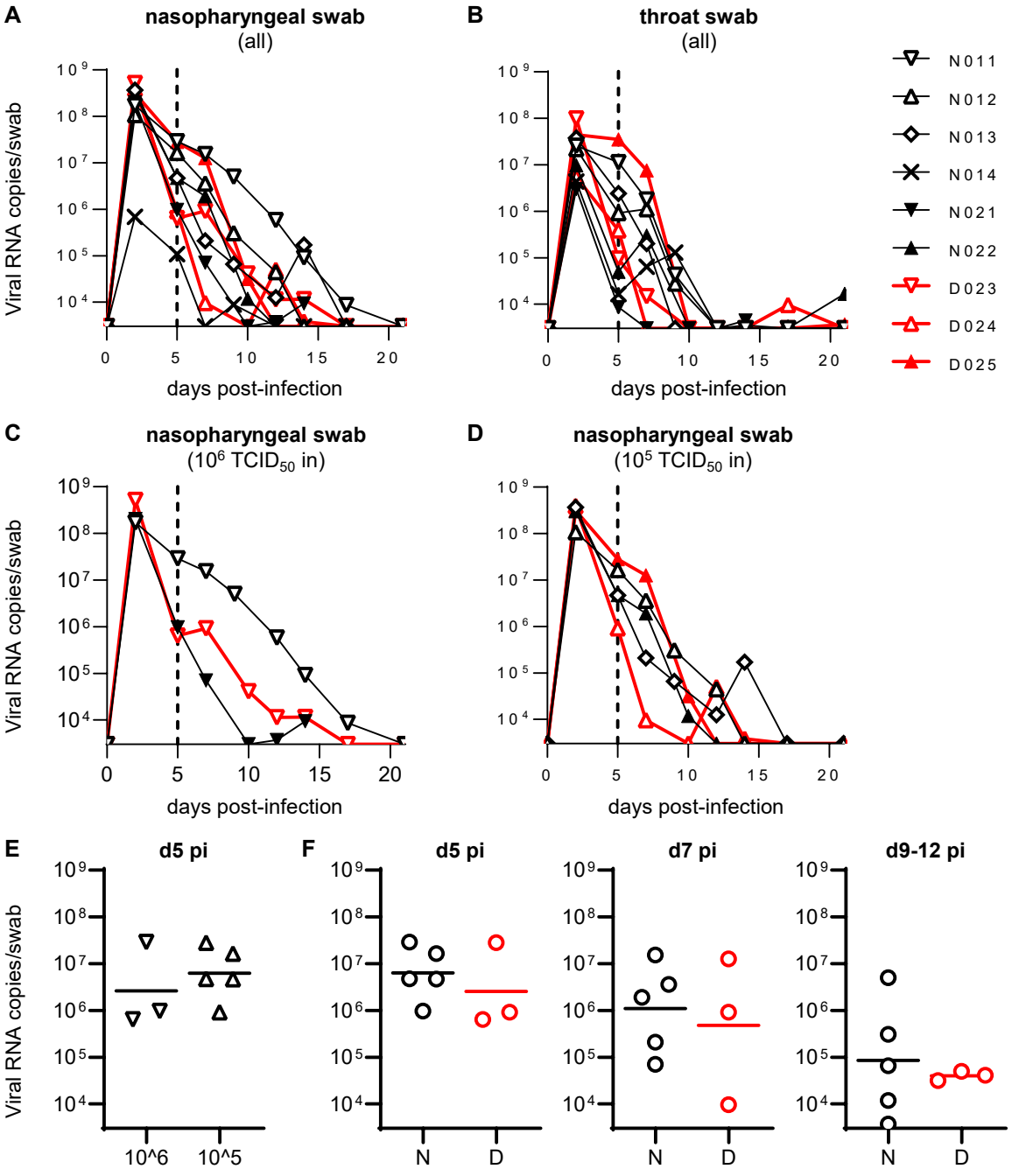
A
nasopharyngeal swab
(all)
Viral RNA copies/swab
days post-infection
B
throat swab
(all)
days post-infection
N011
N012
N013
N014
N021
N022
D023
D024
D025
C
nasopharyngeal swab
(10^6 TCID50 in)
Viral RNA copies/swab
days post-infection
D
nasopharyngeal swab
(10^5 TCID50 in)
days post-infection
E
d5 pi
Viral RNA copies/swab
10^6
10^5
F
d5 pi
d7 pi
d9-12 pi
N
D

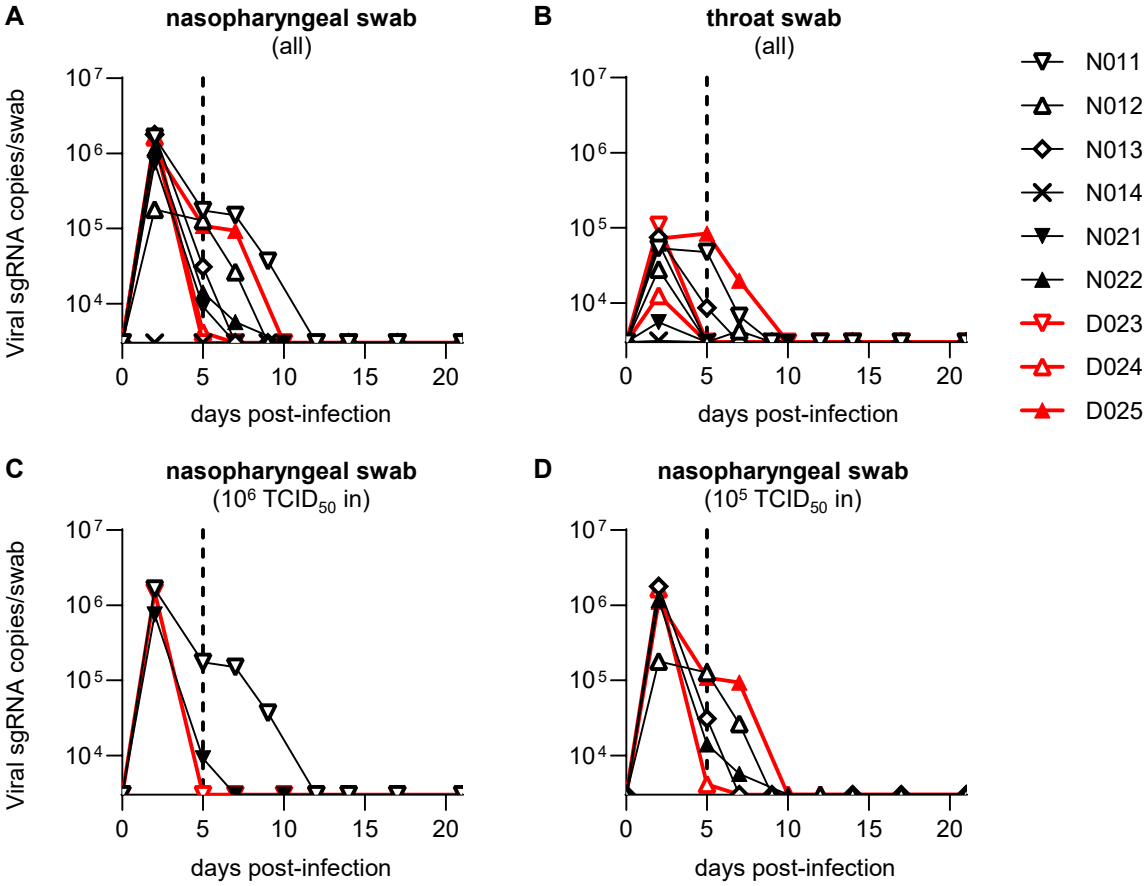
A
nasopharyngeal swab
(all)
B
throat swab
(all)
C
nasopharyngeal swab
(10^6 $TCID_{50}$ in)
D
nasopharyngeal swab
(10^5 $TCID_{50}$ in)
Viral sgRNA copies/swab
10^7
10^6
10^5
10^4
0
5
10
15
20
days post-infection
N011
N012
N013
N014
N021
N022
D023
D024
D025

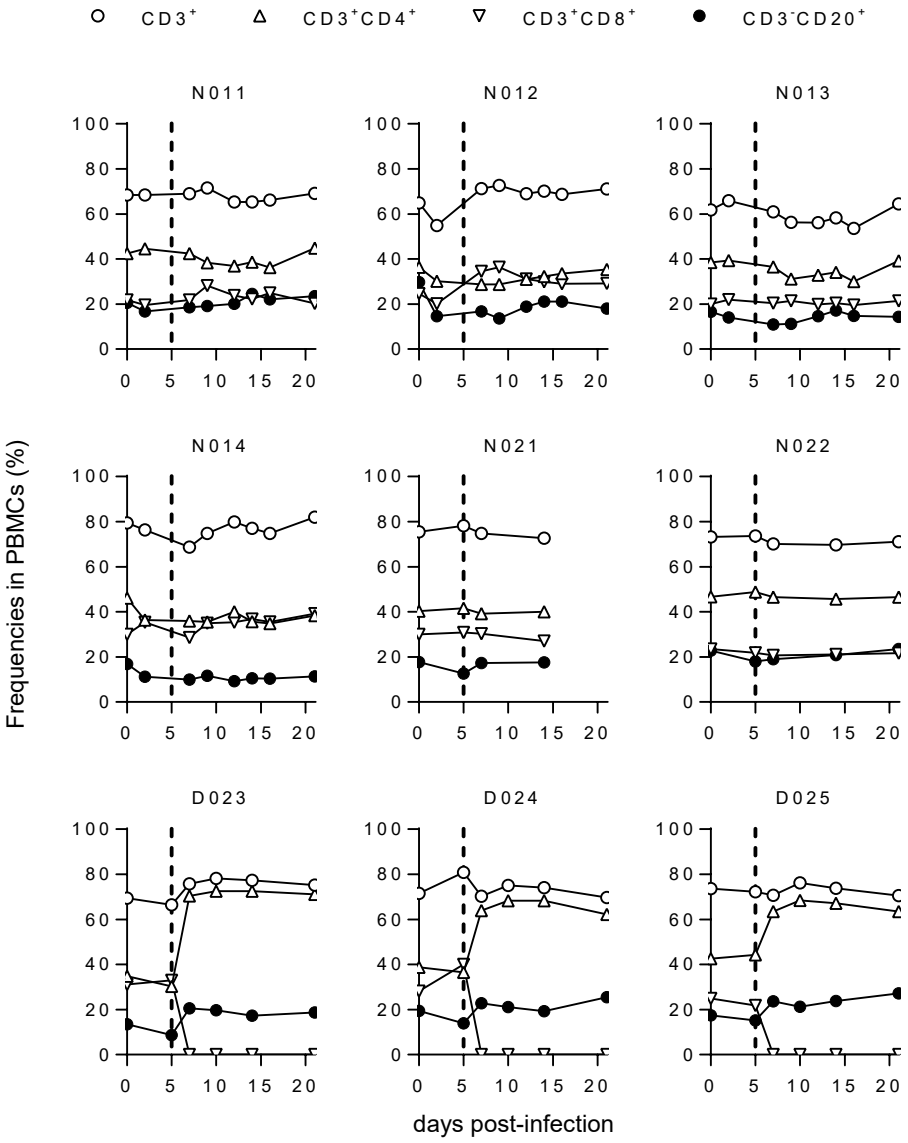
CD3+
CD3+CD4+
CD3+CD8+
CD3-CD20+
N011
N012
N013
N014
N021
N022
D023
D024
D025
Frequencies in PBMCs (%)
days post-infection

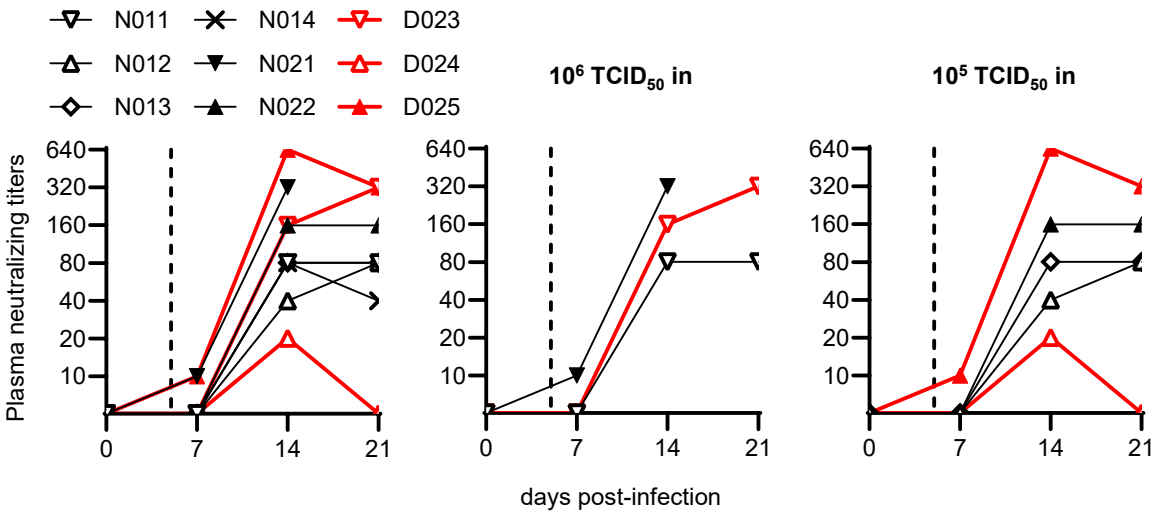
N011
N012
N013
N014
N021
N022
D023
D024
D025
10^6 TCID$_{50}$ in
10^5 TCID$_{50}$ in
Plasma neutralizing titers
640
320
160
80
40
20
10
0
7
14
21
days post-infection

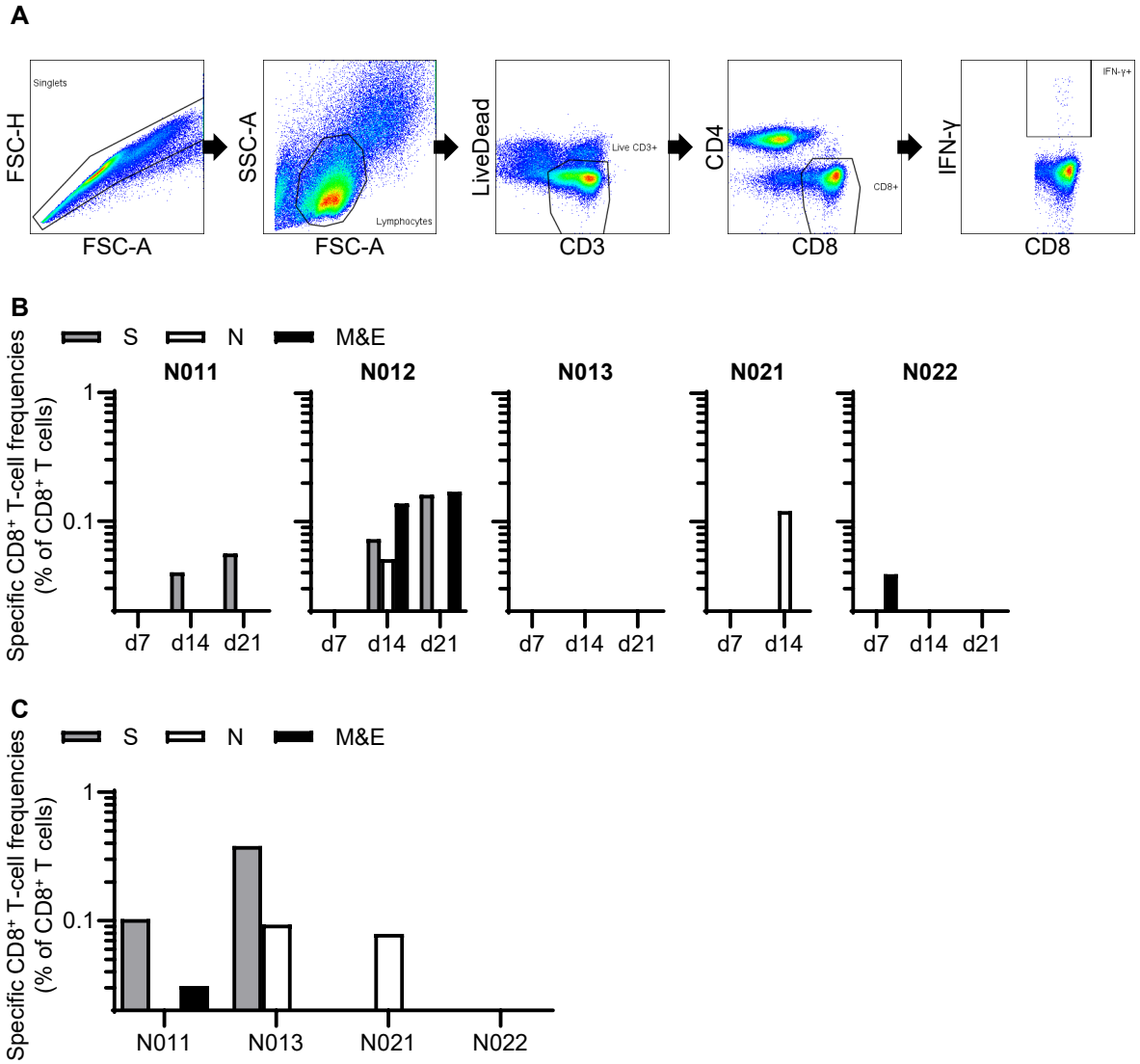
A
Singlets
FSC-H
FSC-A
SSC-A
Lymphocytes
FSC-A
LiveDead
Live CD3+
CD3
CD4
CD8+
CD8
IFN-γ
IFN-γ+
CD8
B
S
N
M&E
N011
N012
N013
N021
N022
Specific CD8+ T-cell frequencies (% of CD8+ T cells)
1
0.1
d7
d14
d21
C
S
N
M&E
Specific CD8+ T-cell frequencies (% of CD8+ T cells)
1
0.1
N011
N013
N021
N022